



Separation of the retinal vascular graph in arteries and veins based upon structural knowledge

Kai Rothaus*, Xiaoyi Jiang, Paul Rhiem

Department of Mathematics and Computer Science, University of Münster, Einsteinstrasse 62, D-48149 Münster, Germany

ARTICLE INFO

Article history:

Received 24 October 2007

Received in revised form 14 February 2008

Accepted 23 February 2008

Keywords:

Retinal vascular graph

Artery

Vein

Constraint satisfaction problem

Constraint propagation

ABSTRACT

The vascular structure of the retina consists of two kinds of vessels: arteries and veins. Together these vessels form the vascular graph. In this paper, we present an approach to separate arteries and veins based on a pre-segmentation and a few hand-labelled vessel segments. We use a rule-based method to propagate the vessel labels through the vascular graph. The anatomical characteristics of the vessels on the retina are modelled as a dual constraint graph. We embed this task as double-layered constrained search problem steered by a heuristical AC-3 algorithm to overcome the NP-hard computational complexity. Results are presented on vascular graphs generated from manual as well as on automatic segmentation.

© 2008 Elsevier B.V. All rights reserved.

1. Introduction

In the last years retinal image analysis becomes a popular research field. Mainly, this trend is advanced by three reasons: (1) retinal images can be produced and distributed with low time and financial costs, (2) the objects on a retina are strong indicators for the presence of some frequently occurred pathologies, and (3) an interesting class of image analysis tasks (vessel segmentation, detection of pathological objects, quantification, etc.) arise in dealing with the retina. Therefore, methods for analysing retinal images have a high relevance in the sense of commercial, medical, and computer scientific aspects. An open problem is the classification of vessels as arteries or veins.

In Figs. 9–13 typical retinal images are depicted. The anatomical structure of the retina is dominated by the vasculature. At the optical disc, which is visible as bright roundish area with a relatively definite diameter of 3.5 mm, the artery 'centralis retinae' intrudes into the eye-ball. At the point of origin this main artery has a calibre of 0.1 mm and branches on the retina at first into a main arch and afterwards into several segments. While branching, the vessels become thinner until they are invisible as capillaries. At the central, darkest area on the retina without any visible vessels the macula is placed, which is the point with the highest density of light receptors. The vein structure is also tree-like, that means without anastomosis (i.e. reconnections).

The retinal vessels are important landmark structures and have themselves a high diagnostic impact. Therefore, there exist various

methods to segment or track the vessels on the retina [1–6]. Another application of vessel segmentation algorithms is a pre-processing prior to the segmentation of pathological objects-like drusen, micro-aneurisms, hard exudates or cotton-wool spoons [7–10]. But some pathologies affect the vessels directly. An increased tortuosity of the arteries is a high indicator of a raised blood pressure. Another measure is the AV-Ratio, which is the ratio of artery to vein calibres (see Wang et al. [11]). Since arteries and veins are differently affected, it is of strong medical interest to have computer-aided methods to classify retinal vessels as arteries or veins [12].

In this work, we present a semi-automatic method to propagate a user-classification through the vascular graph. In this process, we label each vessel segment as artery or vein, respectively. This process can be applied after any proper vessel segmentation algorithm. The focus of this work is not to present a new segmentation but we rather assume that the vascular structure is already segmented suitably. More precisely, we assume a segmentation of a retinal image in form of a binary image, where 1 represents a vessel pixel (object) and 0 any other (background).

The automatic classification of single vessels is still an open task in the retinal image processing. Veins and arteries visually differ in shape, colour and texture. The problem is that such dissimilarities affect only the main vessels and strongly vary dependent on patients, and locations on the retina. Within one retina image there is a high variation in colour, which is caused by inhomogeneous light reflecting due to the spherical surface. Furthermore, the retina of different patients may have varying colours.

Simo and de Ves [13] proposed a Bayesian classifier for pixels to distinguish between arteries, veins, the fovea and the retinal background using image information.

* Corresponding author. Tel.: +49 251 8338448.

E-mail address: rothaus@uni-muenster.de (K. Rothaus).

Chrástek et al. [14] use the local contrast of the red-channel to distinguish between arteries and veins of the main vasculature (near the optical disc). Additionally, they use anatomical features of the vasculature, which we will describe in the next section in detail, to propagate the knowledge during their vessel tracking method. Due to the restriction to a relative small area, their extracted vasculature is rather incomplete and oversegmented. In contrast to them we work on a vessel segmentation which is stronger connected and does not consist of so many connected components like the segmentation which is produced by Chrástek et al. [14]. Thus, we are able to benefit from the anatomical features to a larger extent. Another method is published by Pál et al. [15], who use a neural network with the vessels' cross-profile as input layer to classify arteries and veins. Furthermore, Grisan and Ruggeri [16] have presented a nearest neighbour classifier based on the local colour and contrast of the vessels.

An early approach on vessel classification is published by Akita and Kuga [17]. They use a structure-based relaxation scheme to propagate the artery/vein labelling. Therefore, a network of conditional probabilities is modelled on the vascular graph. These probabilities influence each other and are updated in an iterative way until a stable state is achieved. Thereby, the structure of the vascular graph is kept fixed. Our approach is different from the one of Akita and Kuga [17] in that we make hard decisions. That means, we do not model a probability for the vessel segments to be an artery or vein. In contrast we assign a unique label to a vessel, but rating the plausibility of the extracted network. In case of a conflict the structure of the vascular graph is changed in a suitable way to correct segmentation errors (to some degree) and find a consistent interpretation of the whole vascular graph. Note that [17] is the only structure-based method for separation of veins and arteries in retinal images which we are aware of.

Methodically, our work is similar to the method published by Martínez-Pérez et al. [18] in the way how the vascular sub-trees are extracted. While Martínez-Pérez et al. basically are interested in computing geometrical and topological properties of single vessel segments and sub-trees, we focus in this work on the vascular structure itself. Possibly, our method could be used as an extension for the method of Martínez-Pérez to reduce the number of interactions.

Graph-based approaches are relatively rare in the field of retinal image analysis. Beside Akita's and Kuga [17], there exists a Bayesian approach of Thönnies et al. [19]. They propose an EM-algorithm to iteratively explore a vasculature graph by a random walker technique. Thereby, a random decision corresponds to a graph manipulating operation: join/divide trees, deleting/adding trees, deleting/adding branches, and move nodes to another location. Aguilar et al. [20] present a graph matching algorithm for retinal image registration and mosaicing. Furthermore, the extracted graphs are used to compute a spectral vascular characterisation of vessel network on a retina.

The remainder of this paper is organised as follows. In Section 2, we specify and formalise the problem of separating the vascular graph under anatomical aspects. Subsequently, our algorithm is presented (Section 3) and exemplary results are shown (Section 4). We conclude this work by discussing the performance of the results and giving an outlook on our future work (Section 5).

2. Formal problem specification

In this section, we firstly describe the anatomical features of the vascular structure on the retina. After this we use these criteria to formalise the problem of labelling the vessels as arteries or veins based on the extracted structure.

There are two different kinds of vessels on the retina. The arteries transport oxygenated blood from the heart and the veins discharge the blood back to the heart. We utilise two important anatomical characteristics of these structures:

- (1) The visible vascular structure is physically cycle-free (although its projection onto the 2D image plane becomes a vascular graph with cycles). One artery enters at the optic nerve head into the interior of the retina and branches without any reconnection (i.e. without anastomosis). The same is true for veins.
- (2) At vessel crossings, where one vessel courses over another, only different vessel types are involved. More precisely, an artery could never cross another artery and the same apply accordingly for veins.

Furthermore, the vessels can be distinguished by shape, colour and texture features. Arteries are significantly thinner, have a lighter red appearance and show a clearer visible central light-reflex as veins. In this work, we concentrate our efforts on separating arteries and veins only by the structure of the network on basis of the above-mentioned anatomical characteristics. In recent years there are some works on classifying arteries and veins on the visual features [13–16]. The problem arising in such methods is that these features are only present clearly for the major vessels and sometimes after the first branching on the retina. The objective in this work is to investigate the potential of using additional structural features.

2.1. Graph-based representation

We compute a graph representation of the vasculature in a straightforward way as follows. The precondition of the proposed approach is the segmented vascular structure (Fig. 1(b)). Thereby, a binary image of the same size as the input image of a retina represents the segmentation. Exactly all pixels, which are classified as vessels, are stated with one.

Firstly, we apply a sequential skeletonisation procedure that produces an 8-connected skeleton (see Fig. 1(c)). Maintaining the

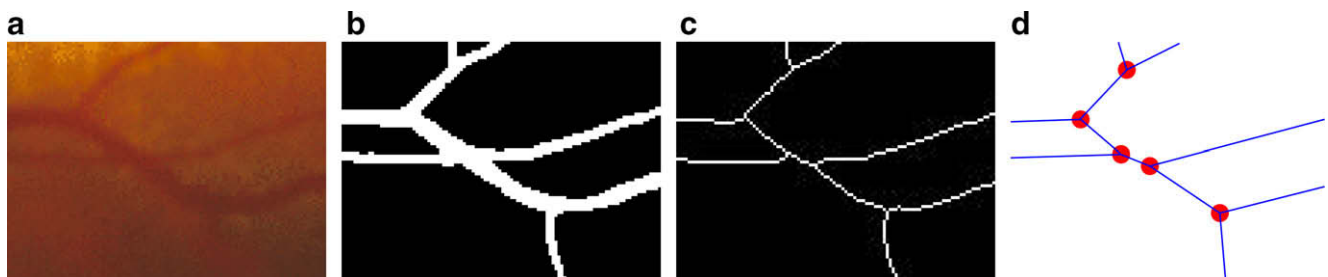


Fig. 1. (a) Inverted original; (b) segmentation; (c) skeleton; (d) vascular graph.

connectivity we delete the segments' boundary iteratively until only one pixel thick curves remain. Once the skeleton is calculated the transformation into a graph \mathcal{G} is straightforward. Because of the vessels' anatomical structure the vertices of \mathcal{G} can only have degree 1, 3 or 4. In contrast to Martínez-Pérez et al. [18] we do not distinguish between the type of vertices on the image analysis level but on anatomical aspects of the vascular structure.

Let us assume that we can represent the vessels as curvilinear segments s_i , which could branch and cross. We construct a planar graph $\mathcal{G} = (\mathcal{E}, \mathcal{V})$, where each edge $e_i \in \mathcal{E}$ ($1 \leq i \leq m$) corresponds to a vessel segment s_i in a one-to-one relation. The nodes v_j ($1 \leq j \leq n$) of the graph represent the branches or crossings of vessel segments and are of degree three (branches) or four (crossings). Additionally, there are nodes of degree one, where a vessel segment ends. If two vessels cross each other, both are splitted in two vessel segments represented by two edges. Thereby, the opposite segments form one vessel segment pair of the same type in each case.

2.2. SAT-problem description

The problem we are faced with is to find a consistent labelling $L(s_i) := L_i$ of all vessel segments s_i in arteries $L_i = a$ or veins $L_i = v$. One can define a rule for a consistent labelling at each vertex v_j depending on its degree: In the case that v_j is a branch, we have three vessel segments with corresponding graph edges e_1, e_2 and e_3 of same type connecting at a node v (see Fig. 2(left)). Clearly, all vessel segments should be labelled in the same manner:

$$L_1 = a \iff L_2 = a \iff L_3 = a \tag{1}$$

$$\wedge L_1 = v \iff L_2 = v \iff L_3 = v \tag{2}$$

From the second anatomical characteristic, we know that if v_j represents a crossing, then one of the involved vessels is an artery and the other is a vein. Physically, these vessels do not cross, but one is taking course above the other. Since vessels are relatively straight, we can assume that a diagonally opposed vessel segment pair represents the same physical vessel and hence the segments belong to the same vessel type. This situation is depicted in the Fig. 2(right). Here e_4, e_5, e_6 and e_7 denote the graph edges linked at a node v . Since the two pairs (e_4, e_6) and (e_5, e_7) belong to the same vessel, we can formulate the following two rules (with a more general indexing):

$$L_4 = a \iff L_5 = a \iff L_6 = v \iff L_7 = v \tag{3}$$

$$\wedge L_4 = v \iff L_5 = v \iff L_6 = a \iff L_7 = a \tag{4}$$

In this way, the extracted vascular graph \mathcal{G} leads to a finite set \mathcal{S} of rules.

Note that L_i can be considered as boolean variable, since we can identify the label a with `true` and v with `false`. In a natural way

we get a satisfiability problem in m variables L_1, \dots, L_m . Obviously, the rules (1) and (2) as well as rules (3) and (4) are redundant so that we keep only the rules (1) and (3) in our rule set \mathcal{S} .

2.3. Constrained search problem

The SAT-problem is a special case of constraint satisfaction problems and can thus be solved by standard algorithms-like AC-3 (see e.g. [21]) to overcome the NP-hard computation trap. The variables $\mathcal{L} = \{L_1, \dots, L_m\}$ are constrained by a set \mathcal{C} of binary relations, which are easily extracted from the rule set \mathcal{S} .

Since the variables are assigned to the edges \mathcal{E} of the vascular graph \mathcal{G} (see Section 2.1) and the constraints connect always two variables we get a dual graph $\mathcal{G}' = (\mathcal{L}, \mathcal{C})$, with the nodes represented by the variables \mathcal{L} and the edges represented the binary constraints \mathcal{C} . Fig. 2 depicts the local construction of the dual graph \mathcal{G}' at a crossing vertex (left) and a branching vertex (right). The primary graph nodes (vessel branches or crossings) are visualised by the dots and the primary edges (vessel segments) as solid lines. The diamonds represents the dual graph nodes (vessel labels) and the dashed curves define the dual graph edges (constraints).

Initially, the domain of each variable L is $\text{dom}(L) = \{a, v\}$. In each connected component of the dual graph \mathcal{G}' one vessel label has to be specified as artery or vein by restricting the variable domain explicitly. Otherwise, there would exist two contrary solutions. The specification could be done arbitrarily, but at the end a user should anyhow decide which of the contrary solutions is the correct interpretation. Therefore, a user interaction is absolutely necessary and could be also done in advance. On basis of an initial specification (user defined as well as arbitrary) of few vessels as artery or vein, the domains of the corresponding variables are reduced to a single value.

These constraints can be propagated through the dual graph by preserving the arc consistency. For this task we use an extension of the AC-3 algorithm which is steered by a priority queue instead of a queue (see Section 3.2).

The basic idea in our application is that due to failures in the extracted vascular graph, some extracted relations (equality or inequality) of the variables are wrong. One possible approach to overcoming this problem is to model the probabilities of a constraint c to be an equality $P(c \equiv (L = L'))$ or an inequality $P(c \equiv (L \neq L'))$, similarly as done by Akita and Kuga [17]. In contrast to that idea, the solution which is presented in this work based upon hard decisions to get a consistent labelling of the whole vascular graph. In contradictory situations, when a variable domain becomes empty, we are searching in the graph \mathcal{G} for the reason of the contradiction and fix it by manipulating \mathcal{G} at an adequate position (see Section 3.4).

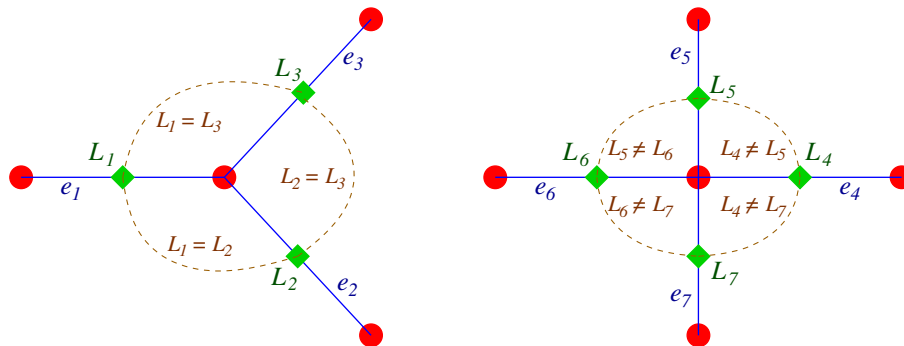


Fig. 2. Construction of the dual graph for a branching (on the left hand) and a crossing (on the right hand).

After solving the SAT-problem each edge of the graph \mathcal{G} is labelled by either a or v . Then, the subset of all edges labelled by a and v corresponds to arteries and veins, respectively. Note that some vessels labels could be still ambiguous. This situation could occur either if a conflict could not be resolved suitably or in the case that a subgraph includes no initially labelled vessel. In the latter case such a subgraph is completely unlabelled and the user should introduce a new vessel label in that subgraph.

2.4. Unsatisfiable vessel labelling

During the segmentation process and the segment identification (e.g. a skeleton algorithm) an erroneous graph representation of the vascular structure may be computed. Typical mistakes are

- (1) splitting of one crossing into two branches;
- (2) missing vessel segment on a side of a crossing;
- (3) falsely detected, i.e. non-existing, vessel segments.

The result of these mistakes is usually a globally unsolvable SAT-problem. For this reason we have to manipulate the graph \mathcal{G} at few selected vertices so that the SAT-problem (Section 2.2) becomes solvable. The selection itself is controlled by the algorithm described in Section 3. We allow the following operations:

- op1** Combining two adjacent branch vertices to one crossing (top row Fig. 3).
- op2** Defining an edge as end segment, which is only connected to one branch or crossing (see middle and bottom Fig. 3).
- op3** Deleting an edge.

Instead of manipulating the graph directly we introduce an auxiliary labelling of vessel segments. To distinguish between the two different types of labelling, we denote the following as *edge labelling* and the discrimination between veins and arteries (Section 2.2) as *vessel labelling*. Possible labels for graph edges are:

- c connection between two branches, which should establish a crossing;
- e artificial end segment, where only one of two vertices is relevant;
- f falsely detected segment;
- n normal segment.

These labellings of edges in the primary graph \mathcal{G} change the interpretation of the graph structure of the edge. Implicitly, a dif-

ferent interpretation affect the constraints at the incident nodes. When we change \mathcal{G} and therewith the interpretation of the vascular structure, we also have to correct the dual graph, which represents the anatomical characteristics of the retinal vasculature. In the following, we describe in brief the implication of changing the labelling of an edge $e \in \mathcal{E}$ from n to c , e or f .

The corresponding graph manipulation operation for introducing a c -label is $op1$. This labelling is only allowed, when e connects two branches and no adjacent edge is labelled with c . In this situation, the dual node in \mathcal{G}' , which corresponds to e is deleted and the four adjacent dual nodes (see Fig. 3, top row) are connected with inequality arcs.

An end segment labelling e (equivalent to $op2$) is only allowed if at most one of the vertices has degree three and the other has degree three or four (see Fig. 3, middle and bottom row). The manipulation of the dual graph depends on the degree of this second vertex. In the case of degree 4, the vessel corresponding to e is supposed not to be physically connected to the other vessel at the branch. Therefore, the rules which are introduced by this branch are causeless and the equality arcs in the dual graph are deleted. In the case that the incident vertices of e are both of degree 3 (bottom row of Fig. 3) one cannot decide the physical connectivity of the vessel segment from the structural perspective. We resolve this decision during our AC-3' algorithm. In the moment, when the domain of the vessel labelling of such an e -labelled edge is reduced, all unused arcs in the dual graph are cancelled.

Noisy segments (label f) are simply thrown away by removing the corresponding node and all incident edges in the dual graph.

2.5. Optimisation task

In Section 3, we will introduce plausibility weights for the vertices and edges of \mathcal{G} . Based upon these ratings we are interested in that solution, which results in a maximum average plausibility. In other words, we search a labelling of graph edges (Section 2.4) so that the resulting SAT-problem (Section 2.2) is solvable and the average plausibility is maximised.

Initially, all vertices v_j of \mathcal{G} are assessed with a plausibility value $w(v_j)$, which should regard the reliability of the assessed rules of v_j . Furthermore, each edge e_i of \mathcal{G} is assigned with the plausibility weight $w(e_i) = 1$ or 0 if the corresponding vessel segment is hand-labelled or not. Based upon the order of applying constraints the weights of the new-labelled segments are updated by a multiplicative propagation scheme (see Eq. (9) in Section 3.2). The optimisation task is then given by minimising

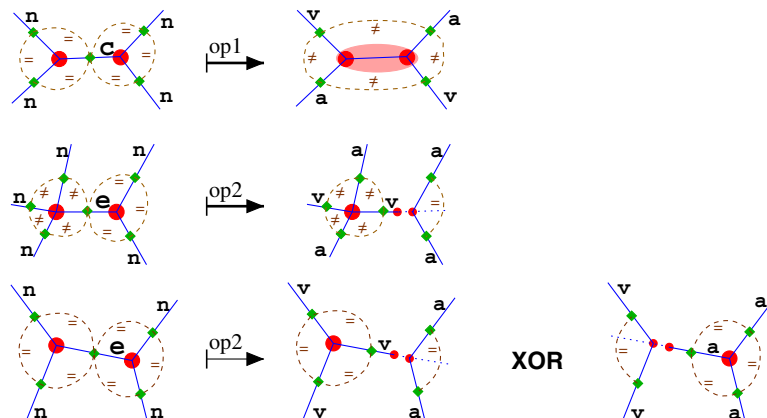


Fig. 3. Implications of: applying op1 by introducing a c -label (top row), applying op2 by introducing an e -label depending on the vertices' degrees (middle row 4/3, bottom row 3/3). Edge labelling on the left, vessel labelling on the right. Primary graph represented by the circle nodes and solid edge-lines; dual graph represented by the diamond nodes and dashed edge-curves.

$$w(\mathcal{G}) = \frac{1}{n} \cdot \sum_{i=1}^n w(e_i) \tag{5}$$

This average plausibility depends on the number of hand-labelled segments and on the order of solving conflicts. Note that in case of an unsolved conflict, wide parts of the graph are left unprocessed and hold the plausibility weight 0.

It is important to keep in mind that $w(\mathcal{G})$ strongly depend on the number and the placement of the hand-labelled vessels and should not be consulted as a quality index of the resulting vessel labelling. We will discuss the interpretation of $w(\mathcal{G})$ and the influence of the hand-labelled vessels in Section 5.

3. Graph separation

The problem we are faced with consists of two layers. The basic layer is the structure of the vascular graph. On this layer graph edges should be labelled with either *c*, *e*, *f* or *n*. This edge labelling defines the constraint set \mathcal{C} , which conditions the second, high-level layer. The dual graph \mathcal{G}' , which has been described in Section 2.3, are used to represent the constraint set \mathcal{C} . With \mathcal{G}' we are enabled to solve the established constrained search problem with an extension of AC-3 by reducing the binary variable domains, so that the arc-consistency is fulfilled.

Our approach is to apply on this higher level a belief propagation and solve conflicts by adjusting the basic layer. More precisely, if contradictory informations are propagated to a vessel segment (competing *a/v*-labelling), we do not propagate the more likely information, but reorganise the structure. This update results in a different, more realistic graph structure.

We use a two-stage approach for the labelling of the vessel segments. In the first stage (Section 3.1), we compute an initial labelling of graph edges. All edges are labelled by *n*, except for those connecting two branches. In the latter case the edge is labelled by either *n* or *c* (indicating a merge of the two branches to build a crossing according to graph manipulation operation *op2*). The decision rule for taking one of the two labels *n/c* is given later in Section 3.1.

The second (higher-order) stage performs the labelling of the vessel segments by a variant of AC-3 (Section 3.2). This algorithm tries to label all vessel segments as arteries *a* or veins *v*. Cycles in the dual graph \mathcal{G}' could cause conflict situations such that a consistent *a/v*-labelling is impossible (Section 3.3). These conflicts are resolved by a backtracking procedure (Section 3.4). The idea is to modify the edge labelling at appropriate edges according to graph manipulation operations *op1-op3*.

3.1. Initial edge labelling

To compute an initial edge labelling, we firstly decide which edges should be labelled with *c*. All other edges are assumed to be normal edges (label *n*). It is important to note that a *c*-label manipulates the graph structure by merging two branch vertices, with degree 3, to a crossing vertex, with degree 4 (see top row in Fig. 3). Therewith, also the dual graph \mathcal{G}' is adjusted accordingly as discussed in Section 2.4.

Let s_c denotes a vessel segment (respectively, a graph edge) to which we want to assign its initial labelling (*c* or *n*). Furthermore, s_1, \dots, s_4 are the other involved vessel segments (see Fig. 4). Two properties help us decide if the two detected branch vertices of s_c actually belong to one vessel crossing:

- P1** The distance d between two branches is relatively small.
- P2** The two segments s_1 and s_3 are roughly collinear, similarly s_2 and s_4 .

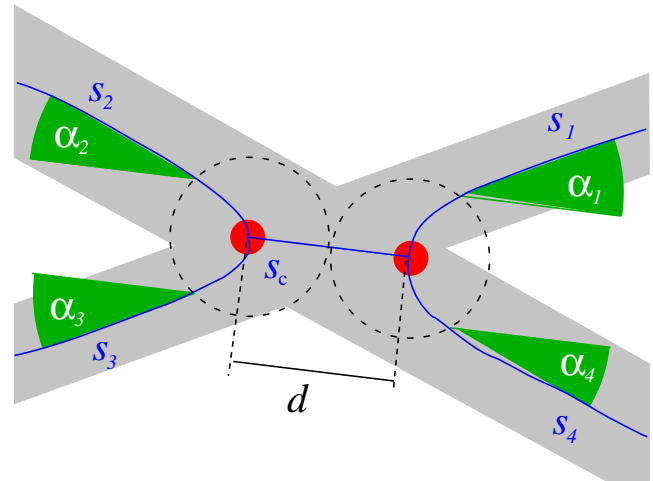


Fig. 4. Weighting of adjacent branches.

We are modelling \mathcal{P}_1 and \mathcal{P}_2 by the following two plausibility functions (see Figs. 5 and 6):

$$\mathcal{P}_1 : [0, \infty) \rightarrow [0, 1], \quad \mathcal{P}_1(d) = 0.95 \cdot \min\{d/d_{\max}, 1\}, \tag{6}$$

$$\mathcal{P}_2 : [-\pi, \pi] \rightarrow [0, 1], \quad \mathcal{P}_2(\beta) = 0.50 \cdot (1 - \cos(\beta)) \tag{7}$$

The constant factor $d_{\max} > 0$ should depend on the resolution of the retinal image. We compute the argument β of \mathcal{P}_2 as

$$\beta = \max\{\alpha_1, \dots, \alpha_4\} \tag{8}$$

Here $\alpha_1, \dots, \alpha_4$ are the inner angles between s_c and s_1, \dots, s_4 (see Fig. 4). If both \mathcal{P}_1 as well as \mathcal{P}_2 are low, we could assume a crossing instead of two branches. We define thresholds T_1 and T_2 and label the segments with *c* if $\mathcal{P}_1 < T_1$ and $\mathcal{P}_2 < T_2$.

The thresholds T_1 and T_2 are determined by optimising this classifier. We hypothesise “segment s_c is a normal vessel” and minimise the beta error on a significance level $\alpha = 0\%$. We have examined 11 vascular graphs with 763 “inner” edges (see Fig. 7). With the conducted thresholds $T_1 = 0.75$ and $T_2 = \mathcal{P}_2(\pi/6)$ all 621 normal edges are correctly labelled with *n*. On the other hand only 25 of 142 crossing edges are falsely labelled with *n*. This corresponds to a beta error of about 17.6% and a total error of about 3.3%.

3.2. Consistent labelling search

In the following an extension of the AC-3 algorithm [21] is proposed, which is controlled by a priority queue $\mathcal{Q} \subset \mathcal{C}$. Note that this

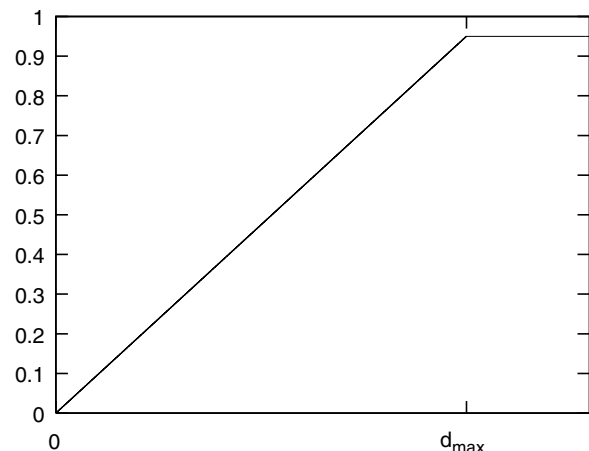


Fig. 5. Plausibility \mathcal{P}_1 of adjacency.

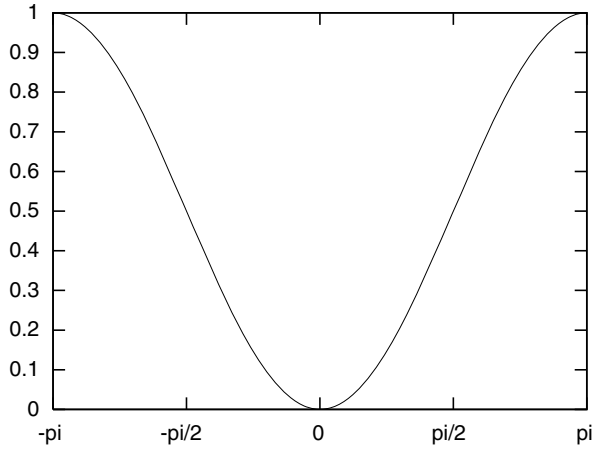


Fig. 6. Plausibility \mathcal{P}_2 of collinearity.

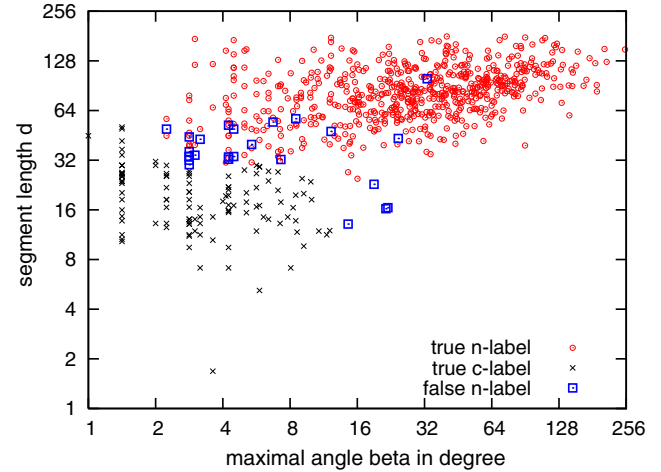


Fig. 7. Specificity of initial labelling.

algorithm is applied on the dual graph. The vertices of this graph corresponds to vessel segments, more precisely their a/v -labels. The edges are the constraints, which are given as the binary relations (equality, inequality).

We presume that \mathcal{Q} initially contains the constraints concerning some hand-labelled vessel segments. Since the vascular structure at the optic disc is very compact, which makes the differentiation of the vessels even for human eyes hardly solvable, we define a circle around the optic disc where the algorithm does not proceed the labelling.

In each step the best constraint $c = (L \sim L')$ is taken out of \mathcal{Q} , where ' \sim ' could be either ' $=$ ' or ' \neq '. In Lemma 1 we will show that each constraint in \mathcal{Q} refers to at least one uniquely labelled vessel (w.l.o.g. $L = a$). Therefore, we can restrict the domain of the other referred vessel label L' , so that the constraint is consistent. If the domain of L' becomes empty, the interpretation of the vascular network is erroneous, and we have to find the reason for the conflict (see Section 3.4). The algorithm stops either if \mathcal{Q} becomes empty or a conflict could not be dissolved. In the set \mathcal{R} the reviewed constraints are stored.

Algorithm 1. AC-3*

Require: Constraint set \mathcal{C} , queue \mathcal{Q} with constraints referring the hand-labelled vessels

```

1:  $\mathcal{R} \leftarrow \emptyset$  // reviewed constraints
2: while  $\mathcal{Q}$  is not empty do
3:    $c = (L \sim L') \leftarrow \text{REMOVE-HEAD}(\mathcal{Q})$ 
4:   // w.l.o.g. let the domain of  $L$  be reduced to one value  $a$  or  $v$ , respectively
5:   if CONSISTENT-LABELLING( $c, L, L'$ ) then
6:      $\mathcal{R} \leftarrow \mathcal{R} \cup c$ 
7:     for all  $c' \in \mathcal{G}'$  incident to  $L'$  do
8:       if  $c' \notin \mathcal{Q} \cup \mathcal{R}$  then
9:         add  $c'$  to  $\mathcal{Q}$ 
10:      end if
11:    end for
12:   else
13:     BACKTRACKING-SEARCH( $c$ )
14:   end if
15: end while

```

To arrange the order of processing, we need a heuristic $H(c)$ that decides “how good” a constraint c is to be treated in the next processing step. For defining the heuristic H we weight the vertices and edges of \mathcal{G} with values $w \in [0, 1]$. The higher a

weight is the more plausible is the interpretation of a vertex or the label of a vessel, respectively. Initially, the weights are defined as follows:

- $w(v) = \mathcal{P}_1(d)$ for a crossing vertex v , where d is the distance to its nearest neighbour;
- $w(v) = \mathcal{P}_1(d) + \mathcal{P}_2(\beta) - \mathcal{P}_1(d) \cdot \mathcal{P}_2(\beta)$ for a branch vertex v and its nearest neighbour vertex (see Fig. 4);
- $w(e) = 1$ if e is a hand-labelled vessel segment (edge).

All vertices of degree 1 and all other edges are initialised with zeros and updated in the labelling process as follows. Let $c = (L \sim L')$ denote the constraint which is processed (i.e. taken out of \mathcal{Q}). Here the domain of L is already reduced to an unique value. Due to the definition of the dual graph, L and L' correspond to vessel segments e and e' in the primary graph \mathcal{G} , which join the common vertex v . We update the weights for the edges e' , if still unlabelled, by

$$w(e') \leftarrow w(e) \cdot w(v) \quad (= H(c)). \quad (9)$$

When the constraint $c' = (L' \sim L'')$ is inserted into the queue \mathcal{Q} , we compute H as:

$$H(c') \leftarrow w(e') \cdot w(v'), \quad (10)$$

where e'' is the edge which belongs to L'' and v' is the common vertex of e' and e'' .

3.3. Localisation of the conflict reason

For simplify the further consideration, we extend the dual graph with one virtual node L_0 and restrict the domain to $\text{dom}(L_0) = \{a\}$. Thereafter, we connect L_0 to each hand-labelled node either with an equality constraint ' $=$ ' in case of a hand-labelled artery or an inequality constraint ' \neq ' in case of a hand-labelled vein. With this extension the initial labelling is embedded consistently in terms of the CSP just by those constraints. The queue \mathcal{Q} in Algorithm 1 can be initialised with these newly introduced constraints referring L_0 . It is important to note that the node L_0 as well as all incident edges, which are introduced by the hand-labelled vessels, must not be changed during the conflict dissolving procedure.

Lemma 1. In the Algorithm 1 the following invariants are always fulfilled for all constraints $c = (L \sim L')$:

1. case ($c \in \mathcal{R}$): $|\text{dom}(L)| = |\text{dom}(L')| = 1$
2. case ($c \in \mathcal{Q}$): $|\text{dom}(L)| = 1 \wedge |\text{dom}(L')| \geq 1$ (w.l.o.g. $|\text{dom}(L)| \leq |\text{dom}(L')|$)
3. case ($c \notin \mathcal{Q} \cup \mathcal{R}$): $|\text{dom}(L)| = |\text{dom}(L')| = 2$

See Appendix for a proof of this Lemma. Lemma 1 demonstrates the operation mode of the AC-3* algorithm. The set \mathcal{R} stores the fulfilled constraints (domains of the referring variables are single-valued), the queue \mathcal{Q} holds the applicable constraints (at least one variable with single-valued). The rest of the constraints are irrelevant at the moment.

This situation is exemplary depicted in Fig. 8. Initially, there is one hand-labelled artery (marked in Fig. 8 with the big *a*). In each pass through the while-loop one constraint is applied and the domain of one variable is assured to be single-valued. In the example of Fig. 8 these constraints are numbered in order of their application. Therewith, the reviewed region (underlaid in grey) is growing and covering the applied constraints. For example the lighter grey region is supplemented during the fifth pass. The queue \mathcal{Q} can be concluded from Fig. 8 as including those constraints (dashed arcs), which partly lie in the reviewed region and partly in the unreviewed. There are two important things to notice. Firstly, a variable domain cannot be empty. In that case a backtracking search undoes the last applications of constraints and the problem is fixed by manipulating the graph structures. The second important fact is, that when \mathcal{Q} is empty, all reviewed constraints in \mathcal{R} are fulfilled by a unique labelling of the referring variables. The following Lemma 2 (see Appendix for a proof) specifies the situation, which causes a conflict.

Lemma 2. Conflict at node L of the dual graph \mathcal{G}' could occur during the AC-3* algorithm if and only if there is a cycle with nodes L'_0, \dots, L'_p with $L = L'_0 = L'_p$ and edges (resp. constraints) $c_i = (L'_{i-1} \sim L'_i) \in \mathcal{R}$ so that the number of inequality constraints ' \neq ' is an odd integer.

Such a conflict causing cycle is depicted in Fig. 8. The constraints numbered with 2, 4, 5, and 6 establish a cycle with only one inequality (constrain number 5) and causes a conflict in the sixth loop pass.

In dead, a conflict causing cycle is present unless any hand-labellings and could be easily located by a pass-consistency check. However, we want to sort all conflict causing cycles implicitly by their order of processing during the heuristical steered AC-3* algorithm.

3.4. Conflict dissolving

Algorithm 2. BACKTRACKING-SEARCH (C)

Require: Constraint c as head of review stack \mathcal{R}

```

1:  $S \leftarrow \emptyset$  // sub-graph to be reviewed again
2: while no conflict cycle  $\mathcal{C}$  is found do
3:    $S \leftarrow S \cup \text{HEAD}(\mathcal{R})$ 
4:    $\mathcal{R} \leftarrow \text{REMOVE-HEAD}(\mathcal{R})$ 
5: end while
6: COMPUTE ( $\mathcal{E}^*$ ) // see Eq. (11)
7:  $\tilde{e} = \arg \min_{e \in \mathcal{E}^*} \{ \mathcal{P}_1(e) + \mathcal{P}_2(e) - \mathcal{P}_1(e) \cdot \mathcal{P}_2(e) \}$ 
8: if  $\mathcal{P}_1(\tilde{e}) < T'_1 \wedge \mathcal{P}_2(\tilde{e}) < T'_2$  then
9:   LABEL( $\tilde{e}$ ) =  $c$ 
10: else
11:    $\tilde{e} = \arg \min_{e \in \mathcal{E}^*} \{ w(e) \}$ 
12:   LABEL ( $\tilde{e}$ ) =  $e$  // or  $\tilde{e}$  if  $e$ -label is impossible
13: end if
14:  $\tilde{L} \leftarrow \text{VESSEL-LABEL}(\tilde{e})$ 
15: while  $\exists (L \sim \tilde{L}) \in \mathcal{R}$  do
16:    $S \leftarrow S \cup \text{HEAD}(\mathcal{R})$ 
17:    $\mathcal{R} \leftarrow \text{REMOVE-HEAD}(\mathcal{R})$ 
18: end while
19: ADJUST-DOMAINS( $S$ )
20: REBUILD-DUAL-GRAPH

```

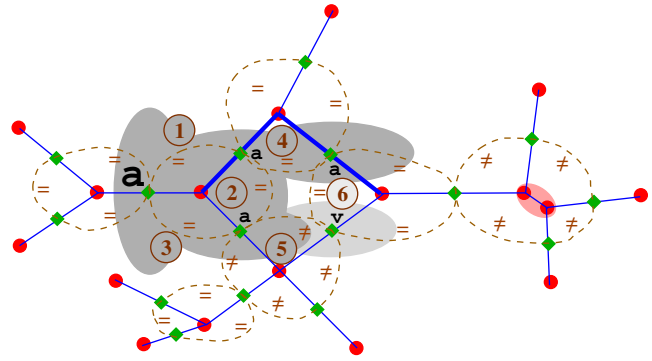


Fig. 8. Exemplary visualisation of: \mathcal{R} , \mathcal{Q} , operation mode of AC-3*, a conflict cycle, and possible conflict solving (see text for details).

During the labelling propagation described above we may encounter a conflict situation, where a domain of variable L becomes an empty set. This happens if a vessel is already labelled as artery or vein and an application of a constraint yields the contrary label.

In such a situation the backtracking procedure is started to find a conflict causing cycle (see Lemma 2). Note that the reviewed set \mathcal{R} can be easily implemented as heap so that the history of constraint application is present. In fact, there might be more than one such cycle, but we consider the shortest one. In the primary graph \mathcal{G} one can identify a corresponding cycle, with edges e'_i (accordantly to L'_i) with $0 \leq i \leq p$ and a node set \mathcal{V}^* . To solve the conflicts we modify the primary graph indirectly by using another auxiliary labelling (Section 2.4).

In general there are two possibilities to resolve a conflict: (1) changing the number of inequalities or (2) cutting the cycle. At first we try to change the number of inequalities. If this is not possible, we secondly try to delete one constraint and consequently cut the cycle. This can be done by introducing an end-segment label e to one edge e'_i . Finally, the algorithm stops (with an unsolved conflict) if actually the introduction of an end-segment is impossible.

Let us consider the first strategy: changing the number of inequalities. Obviously, it is sufficient to add or remove one inequality constrained on the conflict causing cycle. Since we do not want to get in an infinity loop, we only allow to add inequalities. This can be done by relabel the most adequate n -labelled edge with c . The candidate edges \mathcal{E}^* for such a relabelling operation are defined as:

$$\mathcal{E}^* := \{ e = (v, w) \in \mathcal{E} \mid v \in \mathcal{V}^* \wedge \deg(v) = \deg(w) = 3 \wedge \forall \tilde{e} \text{ incident to } v \text{ or } w \tilde{e} \text{ is } n\text{-labelled} \} \quad (11)$$

The most adequate edge is the edge in \mathcal{E}^* which satisfies the constraints $\mathcal{P}_1 < T'_1$ and $\mathcal{P}_2 < T'_2$ and minimises the plausibility $\mathcal{P}_1 + \mathcal{P}_2 - \mathcal{P}_1 \cdot \mathcal{P}_2$. Hereby, $T'_1 > T_1$ and $T'_2 > T_2$ are suitable thresholds. The Algorithm 2 formally describes the backtracking search.

Again reviewing the example in Fig. 8, the edges which could be relabelled with a c -label are marked as thick lines. The edge with the hand-label would minimise the plausibility $\mathcal{P}_1 + \mathcal{P}_2 - \mathcal{P}_1 \cdot \mathcal{P}_2$. However, we protect the hand-labelled edge segments, because a user would hardly label the interior of a crossing. All other edges end at a real or introduced (right, unlabelled sub-graph) crossing node. Due to the anatomical characteristics of the vascular network, such c -labelled edges could not be interpreted suitably.

Comparing the two possible edges for a new c label, we would guess, that the rightmost edge minimises the plausibility. However, it should not be good enough to fulfill the threshold for \mathcal{P}_2 . In that case, an end segment would be introduced.

4. Results

In this section some results of the proposed algorithm are exemplarily presented. Firstly, our concept is proved on manually segmented retinal images of the STARE dataset [1] (see Section 4.1). Subsequently, we demonstrate the applicability on automatically segmented retinal images (see Section 4.2). The user has to label a few vessels as arteries or veins by hand in both series.

The results are presented in two ways. Firstly, we overlay the labelled vessels onto the original retinal image. Here only the skeleton pixels are dyed either in red or in blue (e.g. Fig. 9, left side). The other visualisation of the results is realised within the segmentation of the retinal vessels. Again we use blue and red to distinguish the two vessel types, but now the complete vessel segment is dyed. Furthermore, we indicate the hand-labelled vessels with a darker colour and the unlabelled vessels in white (e.g. Fig. 9, right side). Unsolved conflicts are specified by yellow arrows.

The performance of the algorithm is concluded in Table 1 (manually segmented) and Table 2 (automatically segmented). Beside the identification number of the image, the number of initial c -labels, newly introduced c -labels (conflict resolving), newly introduced e -labels (conflict resolving), resolved and total conflicts are given. In the rightmost column we plot the average weight $w(\mathcal{G})$. As already mentioned, this number should not be used to compare the quality of results for different initial labellings or different retinal images.

4.1. Manually segmented retinal images

The database of our first test series has been established by Hoover et al. [1]. We use their ground-truth segmentation as input for our graph computation procedure, ignore the vessels inside the optical disc and start our AC-3' algorithm with a few hand-classified vessels. In the Figs. 9 and 10 results are depicted, where all conflicts could be treated suitably. Fig. 9 shows the example 'im0002', where we start with two hand-labelled vessel segments and end up with an average plausibility of 0.14 without unsolved conflicts. Initially, there are 13 edges labelled with c and the conflict solver recognises 3 additional c -edges and 1 end segment (label e). The example of Fig. 10 ('im0081' in STARE) starts with 4 hand-labelled segments and 22 c -edges. The graph separation process solves all conflicts by adding 1 end segment and 3 more c -edges. The average plausibility of the result is 0.20. In Table 1 more results on a fair selection of images of the STARE database are presented. Beside the depicted examples 'im0002' and 'im0081' there are four other images (namely 'im0003', 'im0044', 'im0319', and 'im0324') with unsolved conflicts.

Fig. 11(a) ('im0082' in STARE) shows an example, which is more difficult to proceed. If we label 4 vessel segments by hand (Fig. 11(b)) the program stops with an average plausibility of 0.18. Thereby, only 6 of 10 conflicts are solved and two end segments are introduced. The problem arises mainly from the overlaid crossing and branching in the upper right part of the retina (yellow arrows in Fig. 11). If such a situation occurs the user can correct the labelling by introducing more hand-labelled vessels at ambiguous

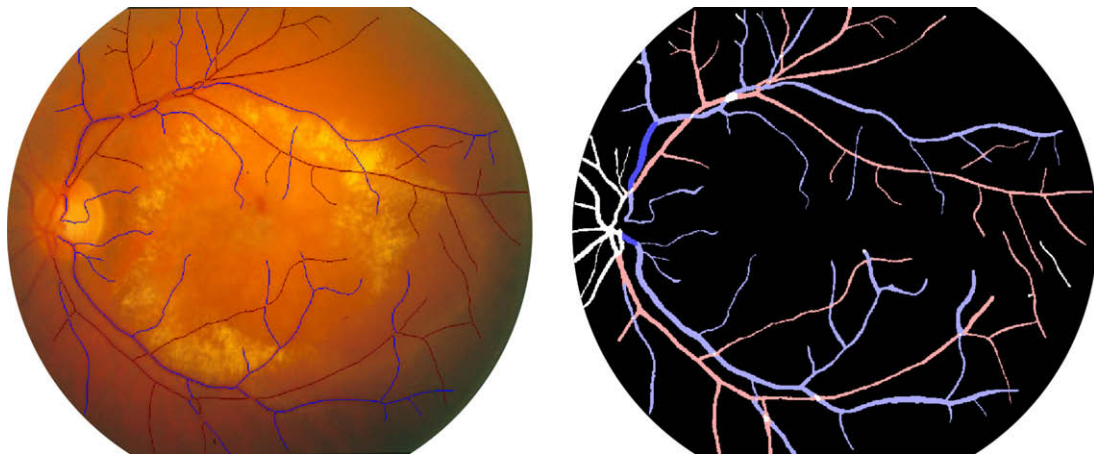


Fig. 9. Vessel classification on manual segmentations 'im0002' in STARE [1]: overlaid on retinal image (left) and dyed segmentation (right).

Table 1
Results on manually segmented images of STARE database [1]

Image ID	Hand labels	Initial c -labels	New c -labels	New e -labels	Solved conflicts	$w(\mathcal{G})$
'im0002'	2	13	3	1	4/4	0.14
'im0003'	4	7	1	0	1/1	0.24
'im0044'	5	9	3	1	4/4	0.23
'im0077'	5	7	8	1	9/10	0.14
'im0081'	4	22	3	1	4/4	0.20
'im0082'	4	17	4	2	6/10	0.18
'im0082'	6	17	4	3	7/9	0.21
'im0162'	7	25	10	8	18/20	0.15
'im0163'	8	16	7	7	14/17	0.20
'im0240'	4	15	3	3	6/7	0.22
'im0319'	3	5	1	1	2/2	0.36
'im0324'	2	5	0	1	1/1	0.22

Table 2
Results on automatically segmented images of DRIVE database [6]

Image ID	Hand labels	Initial c -labels	New c -labels	New e -labels	Solved conflicts	$w(\mathcal{G})$
'06_test'	4	11	2	1	3/3	0.15
'10_test'	4	15	2	1	3/6	0.03
'13_test'	4	14	6	4	10/10	0.04
'14_test'	4	8	3	3	6/7	0.10
'16_test'	6	12	6	0	6/6	0.08
'19_test'	4	16	3	0	3/3	0.04

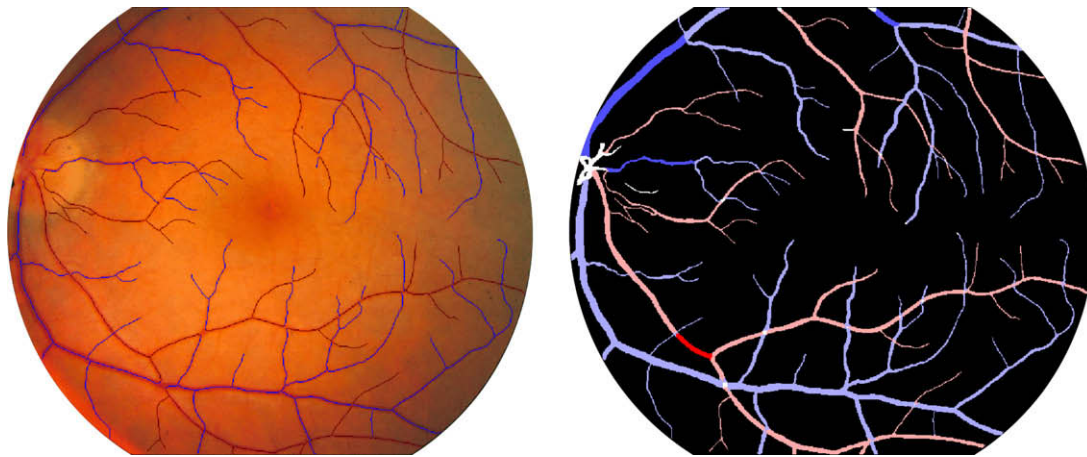


Fig. 10. Vessel classification on manual segmentations 'im0081' in STARE [1]: overlaid on retinal image (left) and dyed segmentation (right).

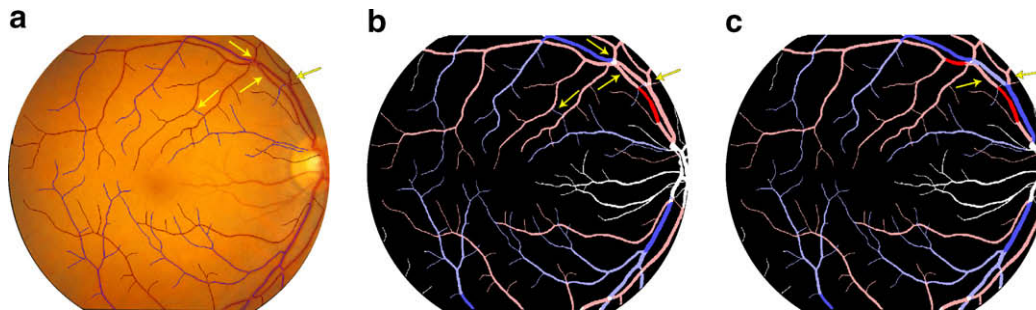


Fig. 11. Problems originated from nearby vessel segments (a) and (b) can be improved by introducing more hand-labelled vessels (c) in 'im0082'.

regions of the retina. But even if we label 6 vessels by hand (Fig. 11(c)) only 7 of 9 conflicts are solved by adding 4 c -labels and 3 e -labels. Note that the higher average plausibility in this case is due to the larger set of hand-labelled vessels. Such situations occur frequently (e.g. Table 1: 'im0077', 'im0082', 'im0162', 'im0163', and 'im0240') and require a user interaction. Thereby, the conflict is presented to the user, who should introduce some more manually labelled vessels near the unclear part of the vascular structure. The computation time to update the result is near real-time, so that the medical expert can directly check the effect of his interaction. Such an user involving procedure is not mischievous, but exactly the kind of assistance which would be expected by medical experts.

Even in the case of an idealised segmentation, some conflicts could not be resolved without further user interaction. Such situation could occur, when the two major vessels (one artery and one vein) wriggle upon each other several times, so that the partitioning of these vessels is ambiguous even in a perfect segmentation (see Fig. 11). Branchings of such twisted vessels are hardly to assign one of them, without involving lower level informations (colour, texture, geometrical features).

Another reason for conflicts is introduced by some smaller vessels, which are partly not visible, due to their low contrast. This could lead to misinterpretation, when the connectivity is lost.

4.2. Automatically segmented retinal images

We also conducted some tests on automatic segmentations. Our observation with such segmentations is that in many cases the connectivity if the vascular graph \mathcal{G} is too weak. Our algorithm needs a sufficiently connected structure to proceed the label propagation. This behaviour is the main reason why the result of our approach on such a small constraint set is correct but not as reliable as for a larger constraint set. The Figs. 12 and 13 present two results on an automatic segmented image of the DRIVE dataset [6] using the publically available vessel segmentation algorithm of Soares et al. [5].

The difficulty of the first example (Fig. 12, image 16 in DRIVE) is due to the fact that some vessels are non-continuously segmented (main vessels at the upper right region of the retina). Overall we get an average plausibility of 0.08, based on 6 hand-labelled vessels. All conflicts are solved by introducing 6 new c -label and

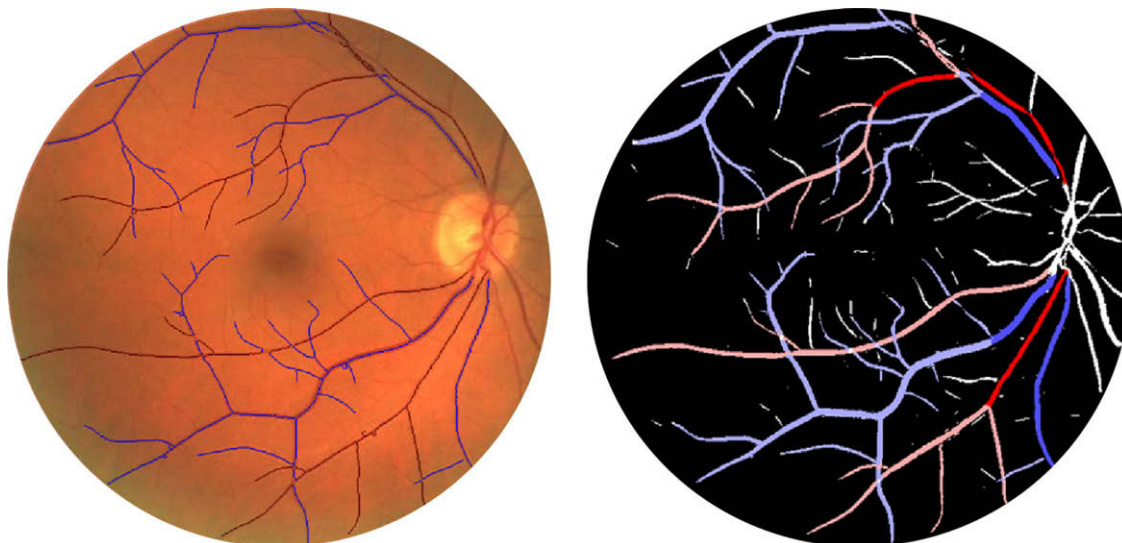


Fig. 12. Vessel classification on automatic segmentation on '16_test' in DRIVE without unsolved conflicts.

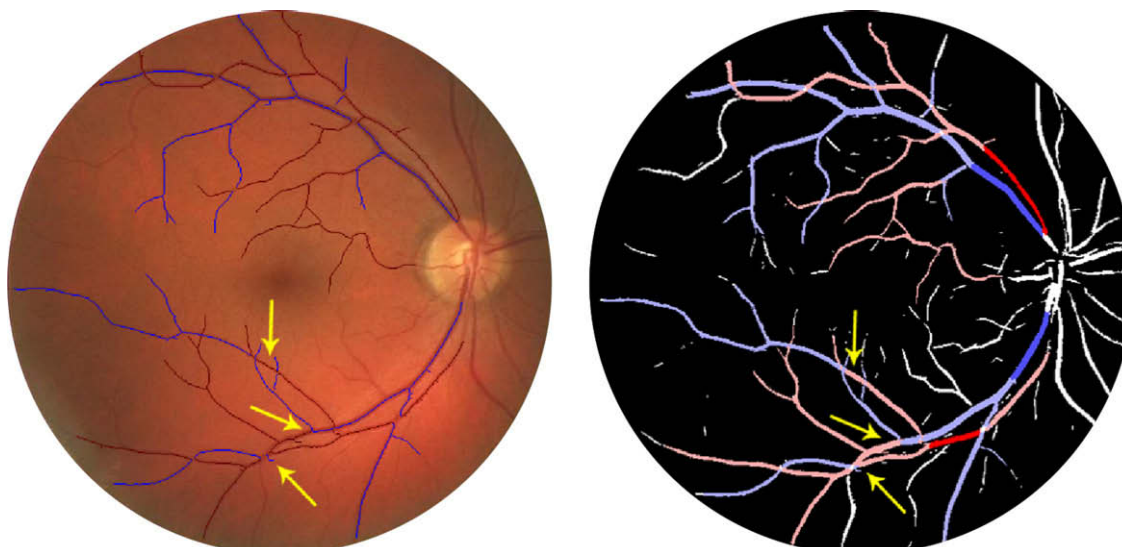


Fig. 13. Vessel classification on automatic segmentation on '10_test' in DRIVE with unsolved conflicts (arrows).

no e -labels. This fact is partly caused by the weak connectivity of the vessel segmentation result, which eases the labelling task since there are fewer constraints compared to a fully connected vascular graph. However, it increases the risk of making erroneous decisions. This effect is shown by the second example (Fig. 13, image 10 in DRIVE), where 3 of 6 conflicts are still unsolved, since the connectivity of the vascular structure is not adequate enough to correct falsely labelled edges. The average plausibility of this example is with 0.03 the lowest of the examples presented in this work. The remaining conflicts all affect the same area of the vascular graph (see Fig. 13). In this subgraphs just a few connections are missed by the segmentation algorithm, to allow an introduction of a c -label. On the other hand there exists some small noisy branches due to holes in the binary segmentation image. The latter kind of noise is the reason, why the average score is lower than in the case of the manually segmented images. The noisy branches often have a low plausibility and results in a rapid decrease of the vessels' weights.

In Table 2 some more examples on automatically segmented images are given. All other retinal images in the DRIVE database are segmented not completely enough to preserve a sufficient structural representation of the vessel network. Remember that the a/v -labelling is propagated on the basis of rules which are assigned to the nodes of the vascular graph \mathcal{G} . If a node is not detected or a vessel is divided into unconnected segments, there are introduced more unconnected subgraphs. In each subgraph the user has to label at least one vessel manually. Such situation is not satisfactory. Currently, we are intending an extension of vessel segmentation algorithms in such a way that the structural features are preserved or reconstructed.

5. Discussion and conclusion

We have presented an automated graph separation algorithm to distinguish between arteries and veins in retinal images. The results on the manually segmented images are promising and prove

the applicability of our concept. A medical expert has to label a few vessels as arteries or veins manually. This user interaction could be avoided by an automatic detection of the optic disc and an automatic classification of close-by dominant vessels.

The performance of our algorithm mainly depends on the quality of the vessel segmentation algorithm. Although we could correct isolated segmentation errors, cumulatively mistakes or non-continuous vessels are still difficult to handle.

On the other side this malpractice offers a chance to locate segmentation errors. If there is a region, where the extracted vessels could not be arranged under anatomical aspects, this is an indication for a segmentation error. Beside the use of such higher level information, we are working on an extended conflict solver, which could delete edges/vessels.

Furthermore, we want to justify our algorithm by a comprehensive quantitative study, in which our results are compared to a ground truth labelling, which has to be established. The ground truth, which is presented by Hoover et al. [1] only define true vessels, but not their type (artery or vein). Moreover, we are interested in an objective, quantitative measure of the achieved quality of a result. The average weight is not useful to compare two resulting labellings because it strongly depends on the number and position of the hand-labelled vessels. With different initial hand-labellings a user can easily produce the same result, but with different average weights.

We have developed an adaptive user interface, which helps physicians to process their analysis in a more efficient way.

We also want to enhance the method by a statistical foundation of the weights. Also a Bayes classifier of the on basis of the two features d (Euclidian distance of the segment end points) and β (maximum angle) should be established. At the moment we do not use the anatomical feature, that the arteries and the veins are cycle free on the retina. This can be modeled by forbidding cycles in the dual graph, which do not include an inequality constraint (beside the cycle, which takes course around one single branch).

Finally, this structural feature approach should be embedded in a more general framework, where we also use shape, texture and colour feature of the vessels to separate veins and arteries. Currently, we are working on a method, in which classifiers on different information levels are combined. Hereby, a higher level classifier could adjust lower level classifiers, by validating the classification results.

In conclusion one can say that the automatic separation of the vascular graph into vein and artery components offers many chances to interpret characteristics of the vessel structure on a higher information level. It could be possible to correct errors on lower levels by a suitable interaction scheme.

Acknowledgments

We thank Adam Hoover et al. and Joes Staal et al. for making their retinal image databases publically available. Furthermore, we thank João Soares et al. for providing their MATLAB code for vessel segmentation. Many thanks to Elena Martínez-Pérez for the fruitful discussions during the GBR-workshop in Alicante, 2007, and last but not least all reviewers for all their helpful suggestions.

Appendix

Proof of Lemma 1. Initially $\mathcal{R} = \emptyset$ and case 1 is trivially valid. The queue \mathcal{Q} contains all constraints referring L_0 and the hand-labelled variables. Since at the beginning L_0 is the only node with a single-valued domain the cases 2 and 3 are fulfilled, too.

Let us assume, the invariants are valid at the beginning of the while-loop. After the removal of the head $c = (L \sim L')$ of \mathcal{Q} the domain of L' is reduced so that the arc-consistency is given with

respect to the relation $L \sim L'$. Since L has a single-valued domain (assumption) and ' \sim ' is either '=' or ' \neq ', the domain of L' is restricted to an unique value or becomes empty. In the latter case the backtracking search undoes the last constraint applications and modify the graphs. In the former case the insertion of $(L \sim L')$ into \mathcal{R} corresponds to case 1 in this lemma.

Finally, all constraints $c' \notin \mathcal{Q} \cup \mathcal{R}$ referring L' are added to \mathcal{Q} . Since L' has now a single-valued domain and the other must have a non-restricted domain this conforms the cases 2 and 3. Concluding, it is proved that the invariants are fulfilled at the end of the while-loop and hence during the whole algorithm. \square

Proof of Lemma 2. Beside the empty domain of L the domains of all $L' \in \mathcal{L}$ are non-empty (Lemma 1). Assumed there is no cycle in the graph $\mathcal{G}_{\text{act}} = (\mathcal{R}, \mathcal{L}_{|\mathcal{R}})$ which contains L , then each path containing L is linear. Since $L_0 = a$ was the only restricted variable at the beginning of Algorithm 1, a consistent (regarding \mathcal{R}) labelling of all other ($L' \in \mathcal{L}_{|\mathcal{R}}$) is possible. Obviously, the conflict is not reasonable and hence could not has been produced by the AC-3* algorithm.

So there must be a cycle which causes the conflict. Let L'_0, \dots, L'_p with $L = L'_0 = L'_p$ denote the cycle nodes and let $c_i = (L'_{i-1} \sim L'_i) \in \mathcal{R}$ represent the cycle edges. Due to Lemma 1, the domain of L'_i is single-valued (beside the empty domain of L_0).

Note that an inequality results in a change of the label. The node L is connected through a constrained path c_i to itself. Since the possible domain of each L'_i is binary, one can resolute the conclusion $L = L$ if there is an even number of inequalities and $L \neq L$ if there is an odd number. Obviously, the conflicts is founded exactly by the latter case. \square

References

- [1] A. Hoover, V. Kouznetsova, M. Goldbaum, Locating blood vessels in retinal images by piece-wise threshold probing of a matched filter response, IEEE Transactions on Medical Imaging 19 (3) (2000) 203–210.
- [2] X. Jiang, D. Mojon, Adaptive local thresholding by verification-based multithreshold probing with application to vessel detection in retinal images, IEEE Transactions on PAMI 25 (1) (2003) 131–135.
- [3] K. Rothaus, X. Jiang, Multi-scale segmentation of the vascular trees in retinal images, in: Proc. 3rd EMBC, 2005.
- [4] E. Ricci, R. Perfetti, Retinal blood vessel segmentation using line operators and support vector classification, IEEE Transactions on Medical Imaging 26 (10) (2007) 1357–1365.
- [5] J. Soares, J. Leandro, R. Cesar Jr., H. Jelinek, M. Cree, Retinal vessel segmentation using the 2-d morlet wavelet and supervised classification, IEEE Transactions on Medical Imaging 25 (2005) 1214–1222.
- [6] J. Staal, M. Abramoff, M. Niemeijer, M. Viergever, B. van Ginneken, Ridge based vessel segmentation in color images of the retina, IEEE Transactions on Medical Imaging 23 (2004) 501–509.
- [7] L. Brandon, A. Hoover, Drusen detection in a retinal image using multi-level analysis, in: MICCAI, vol. 1, 2003, pp. 618–625.
- [8] K. Huang, M. Yan, A local adaptive algorithm for microaneurysms detection in digital fundus images, in: CVBIA, 2005, pp. 103–113.
- [9] W. Hsu, P. Pallawala, M. Lee, K.A. Eong, The role of domain knowledge in the detection of retinal hard exudates, in: CVPR, vol. 2, 2001, pp. 246–251.
- [10] N. Patton, T. Aslam, T. MacGillivray, I. Deary, B. Dhillon, R. Eikelboom, K. Yogesan, I. Constable, Retinal image analysis: concepts applications potential, Progress in Retinal and Eye Research 25 (1) (2006) 99–127.
- [11] J. Wang, G. Liew, T. Wong, W. Smith, R. Klein, S. Leeder, P. Mitchell, Retinal vascular calibre and the risk of coronary heart disease-related death, Heart 92 (2006) 1583–1587.
- [12] M. Larsen, L. Colmorn, M. Bonnelycke, R. Kaaja, I. Immonen, B. Sander, S. Loukovaara, Retinal artery and vein diameters during pregnancy in diabetic women, Investigative Ophthalmology and Visual Science 46 (2005) 709–713.
- [13] A. Simo, E. de Ves, Segmentation of macular fluorescein angiographies a statistical approach, Patter Recognition 34 (4) (2001) 795–809.
- [14] R. Chrástek, M. Wolf, K. Donath, H. Niemann, G. Michelson, Automated calculation of retinal arteriovenous ratio for detection and monitoring of cerebrovascular disease based on assessment of morphological changes of retinal vascular system, in: Proc. IAPR Workshop on Machine Vision Applications, Nara, Japan, 2002, pp. 240–243.
- [15] I. Pál, G. Michelson, G. Zinser, Automatische Bestimmung des Arterie-Vene-Verhältnisses auf Retina-Tomograph-Bildern, in: Bildverarbeitung für die Medizin, 2000, pp. 319–323.

- [16] E. Grisan, A. Ruggeri, A divide et impera strategy for automatic classification of retinal vessels into arteries and veins, in: Proc. 25th Annual IEEE Int. Conf. Engineering in Medicine and Biology Society, 2003, pp. 890–893.
- [17] K. Akita, H. Kuga, A computer method of understanding ocular fundus images, *Pattern Recognition* 15 (6) (1982) 431–443.
- [18] M. Martinez-Perez, A. Hughes, A. Stanton, S. Thom, N. Chapman, A. Bharath, K. Parker, Retinal vascular tree morphology: a semi-automatic quantification, *IEEE Transactions on Biomedical Engineering* 49 (8) (2002) 912–917.
- [19] E. Thönnies, A. Bhalerao, W. Kendall, R. Wilson, A bayesian approach to inferring vascular tree structure from 2d imagery, in: Proc. Int. Conf. Image Processing, 2002, pp. 937–940.
- [20] W. Aguilar, M.E. Martínez-Pérez, Y. Frauel, F. Escolano, M.A. Lozano, A. Espinosa-Romero, Graph-based methods for retinal mosaicing and vascular characterization, in: Proc. Graph-Based Representations in Pattern Recognition, 6th IAPR-TC-15 International Workshop, Alicante, Spain, June 11–13, 2007, pp. 25–36.
- [21] S. Russel, P. Norvig, *Artificial Intelligence: A Modern Approach*, 2nd ed., Prentice Hall International, 2003.





ID	Title	Pages
527170	Separation of the retinal vascular graph in arteries and veins based upon structural knowledge	12

Related Articles



<http://fulltext.study/journal/572>



-  **Categorized Journals**
Thousands of scientific journals broken down into different categories to simplify your search
-  **Full-Text Access**
The full-text version of all the articles are available for you to purchase at the lowest price
-  **Free Downloadable Articles**
In each journal some of the articles are available to download for free
-  **Free PDF Preview**
A preview of the first 2 pages of each article is available for you to download for free

<http://FullText.Study>